JOURNAL OF MAGNETIC RESONANCE **126,** 200–206 (1997)
ARTICLE NO. MN971151

Mechanically Detected Nuclear Magnetic Resonance at Room Temperature and Normal Pressure

Arnd Schaff and Wiebren S. Veeman

Department of Physical Chemistry, University of Duisburg, Lotharstrasse 1, 47048 Duisburg, Germany

Received October 16, 1996; revised February 24, 1997

Mechanically detected magnetic resonance (MMR) is a new technique for detecting electron or nuclear spin signals. All preceding experiments have been carried out in a $<10^{-3}$ Torr vacuum at room temperature or at low temperatures down to 6 K. In this article the first MMR experiments at normal pressure and room temperature are presented. The mechanically detected NMR signals resulted from ammonium nitrate and ammonium sulfate. In addition, techniques for determining T_1 and $T_{1\rho}$ with mechanical experiments were developed. If $T_{1\rho}$ is not more than two or three times smaller than T_1, an inversion-recovery technique, first used for the detection of ^{19}F spins at low temperatures, can be used. It could be shown that this technique also works in principle at room temperature.

INTRODUCTION

Mechanically detected magnetic resonance (MMR) was proposed in 1992 by Sidles (*1–3*). The main idea of the method is to excite a mechanical oscillator, for example, a cantilever known from atomic force microscopy (AFM), by inducing NMR or ESR transitions in a sample near to or connected to the oscillator. By detecting the oscillation of the cantilever by an interferometer (*4*) or a light beam deflection system the presence of spins can be revealed. In the first experiments (Rugar *et al.*) electron spins (DPPH) and proton spins (ammonium nitrate) were detected at room temperature and at a pressure below 10^{-3} Torr (*5, 6*). Other experiments have been performed at temperatures down to 6 K with ^{19}F spins (*7*).

MMR could be a powerful new technique with an extremely high sensitivity that allows high-resolution imaging of electron or nuclear spin densities. First experiments have already shown that the resolution is better than that in conventional NMR imaging (*8, 9*). It seems to us that one can pursue two different goals in the further development of MMR. The first goal could be to enhance the sensitivity of the method, ultimately perhaps leading to single-spin detection. Then, without doubt, vacuum experiments at low temperatures are needed to enhance the quality factor of the mechanical oscillator, to reduce the thermal noise, and to make the magnetization as high as possible. Another aim could be to develop a routine high-resolution technique for the spin-density reconstruction of samples such as polymer materials or biological samples. Especially biological samples, like living cells, would require the possibility of measurements at room temperature and normal pressure. Therefore we are trying to develop MMR under these conditions.

With MMR only certain regions in the sample contribute to the signal. This can be used to map the spin density of the sample, turning the instrument into a magnetic resonance microscope. Such experiments have already successfully been performed (*8*). In heterogeneous materials (polymers, biological cells) one can expect a wide range of values for the various spin relaxation times. This can lead to a T_1- or $T_{1\rho}$-weighted map of the sample and we therefore also show here how to combine MMR with T_1 or $T_{1\rho}$ selection.

Rugar *et al.* (*6*) used the fast adiabatic passage (*10*) method to modulate the NMR magnetization in the MMR experiment. This technique requires a long $T_{1\rho}$ for optimum sensitivity, a $T_{1\rho}$ value much longer than the values usually found in samples at room temperature. For short $T_{1\rho}$ values excitation methods other than repetitive fast adiabatic passages need to be investigated and we report one possibility. Here only the ratio between T_1 and $T_{1\rho}$ is important for the signal, not the absolute values.

EXPERIMENTAL

The apparatus we use for our experiments is shown schematically in Fig. 1. As the magnetic field source, a conventional wide-bore (7 cm) 4.7 T NMR magnet is used. The sample is mounted on the tip of a commercially available silicon nitride cantilever by gluing it with a conventional two-component glue with the help of a light microscope. In the large field the magnetization of an iron particle (cylinder diameter = 0.7 mm, length 4.1 mm) right above the sample is saturated and the spins in the particle are oriented according to Curie's law. Due to the large field gradient produced by the iron particle (distance particle − sample ≈ 0.7

1090-7807/97 $25.00

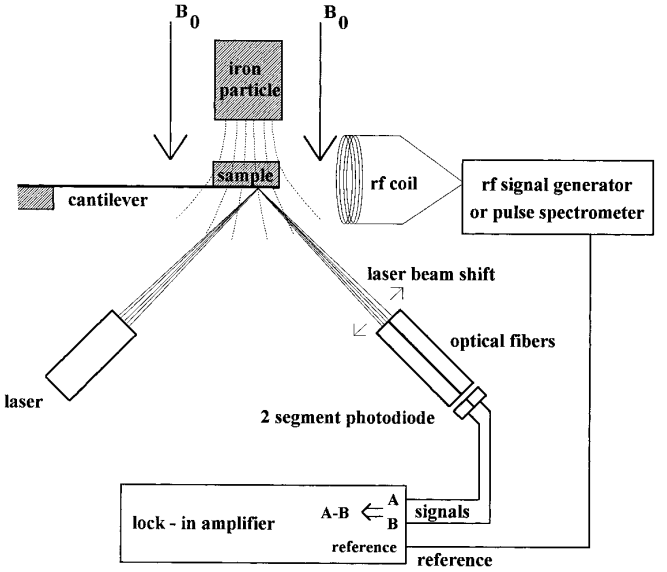

FIG. 1. Schematic drawing of the MMR apparatus. The sample is mounted on the tip of an AFM cantilever. Above the sample is an iron particle to produce a field gradient. The spin magnetization parallel to B_0 is modulated by RF excitation. A laser beam deflection system is used to detect cantilever vibrations. The diode signals are measured with a lock-in amplifier that is locked to the cantilever resonance frequency.

mm) and due to the polarized spins in the sample, a magnetic force acts on the cantilever. The field gradient $\delta B_z/\delta z$ at the site of the sample was $\approx$500 T/m. The z component of the force (neglecting x and y field components) is given by

$$F_z(t) = \frac{\delta}{\delta z}\,[m_z(t)B_z], \qquad [1]$$

where $m_z(t)$ is the time-dependent sample magnetization and B_z is the z component of the magnetic field at the side of the sample. The RF excitation is created by a continuous-wave RF source that is capable of frequency modulation. Possible modulation patterns are ramps, sinusoidal modulations, and sums of both. The frequency-modulated RF excitation can cause a time-dependent sample magnetization $m_z(t)$ and therefore a time-dependent force in the z direction. When this time dependence corresponds to the resonance frequency of the cantilever, an oscillation will result. The amplitude of the oscillation is, among other factors, determined by the quality factor of the resonator (50–100). The deflection of the oscillating cantilever is detected by a light beam deflection system. A laser beam is reflected by the back side of the cantilever to a two-segment photodiode. The diode signal forms the input signal for a lock-in amplifier, the reference signal of which is equal to the resonance frequency of the cantilever. Compared to the interferometer used by Rugar *et al.*, the beam deflection system has the advantage that deflections larger than the light wavelength of the laser can be detected.

The different modulation schemes of the RF excitations are shown in Fig. 2. Although, as we will see, the real situation is more complicated, the general idea is to start the experiment with a frequency far away from the Larmor frequency of the spins one wants to excite. Then the frequency is swept to the Larmor frequency of the spins (Fig. 2a). Under adiabatic conditions the magnetization follows the effective field in the rotating frame,

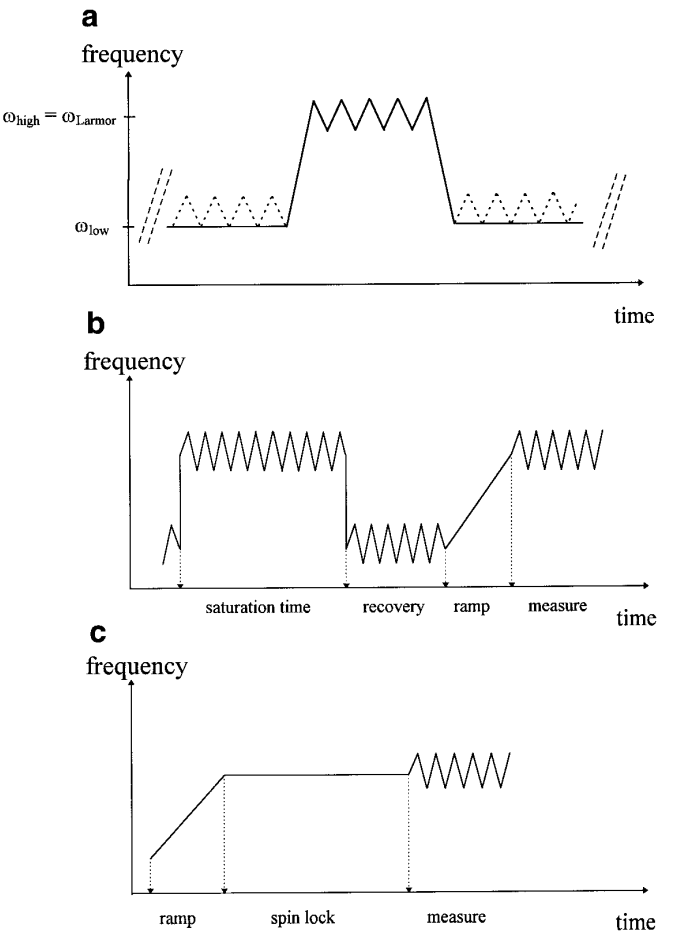

FIG. 2. Modulation patterns used for our MMR experiments. In (a) the general idea of the method is depicted. The RF is swept from frequency ω_{low} to frequency ω_{high} (equal to the Larmor frequency of the spins to be detected) and then, after a measurement period, swept down again. In addition to these frequency ramps, the RF is FM modulated, either only during the measurement period or continuously (dotted curve). The MMR signal can be detected after the first ramp and/or after the second (see text). The spin–lattice relaxation time T_1 is determined with scheme (b). Initially, with $\omega = \omega_{high}$ the magnetization of the spins involved is destroyed completely. Then the spins can repolarize during the variable recovery period, which is followed by the modulation pattern (a). For the $T_{1\rho}$ measurements, pattern (c) is used. The RF without FM is first ramped up to the Larmor frequency. Then the magnetization decays in the spin-lock period, after which the measurement is performed.

$$\mathbf{B}_{\text{effective}} = B_{\text{RF}}\hat{\mathbf{x}} - \frac{\Delta\omega(t)}{\gamma}\hat{\mathbf{z}}, \qquad [2]$$

where B_{RF} is the amplitude of the RF field, γ is the gyromagnetic ratio (2.68×10^8 rad s^{-1} T^{-1} for protons), and $\Delta\omega(t)$ represents the offset frequency. After the ramp the magnetization has made a half-adiabatic passage and is perpendicular to the large dc field. Then the FM modulation

$$\Delta\omega(t) = \Omega \sin(\omega_c t + \varphi) \qquad [3]$$

takes care of repetitive adiabatic fast passages through resonance, generating an oscillating z magnetization. Here, Ω is the modulation depth, $\omega_c/2\pi$ is the cantilever resonance frequency, and φ is a phase angle. This makes the cantilever oscillate with an amplitude proportional to the magnetization of the excited spins. In this description it is also possible to modulate the frequency for the entire time (indicated by the dotted curve in Fig. 2a), because the modulation does not affect the magnetization when the carrier frequency is far away from the Larmor frequency.

In reality the situation is somewhat more complicated because not all the spins in a sample have the same Larmor frequency. Due to the field gradient of the iron particle, spins in different locations in the sample have different Larmor frequencies. In Fig. 3 the range of resonance frequencies of the sample is shown by a rectangle. The RF excitation is indicated with two frequency bands (due to the FM modulation), centered at a high (ω_{high}) and a low frequency (ω_{low}). Depending on the values of ω_{high} and ω_{low}, relative to the sample frequency range, one can distinguish three situations. Figure 3a depicts the situation where only ω_{high} corresponds to some of the Larmor frequencies. Here a signal can be expected after the first ramp. In Fig. 2b both ω_{high} and ω_{low} equal resonance frequencies of spins in different locations of the sample. Now a signal can be expected after each of the ramps, although the second signal may be smaller than the first because the irradiation before the first ramp has saturated the spins with a Larmor frequency $\approx\omega_{\text{low}}$. Only when the spin–lattice relaxation time T_1 is not much longer than the time between the two ramps can a second signal be observed.

In our MMR experiments the frequency ramps are ±500 kHz during 200 ms. The time between the ramps, the measurement time, is 5 s. The FM depth Ω is ±150 kHz. The resonance frequency of the loaded cantilever varies, depending on the weight of the sample ($1–2 \times 10^{-6}$ g) and the spring constant, between 786 and 527 Hz.

All experiments were performed at normal pressure, so we could not take advantage of the gain in the signal-to-noise ratio when measuring in a vacuum. The spectral density of the force noise, assuming only thermal noise, is given by (*6*)

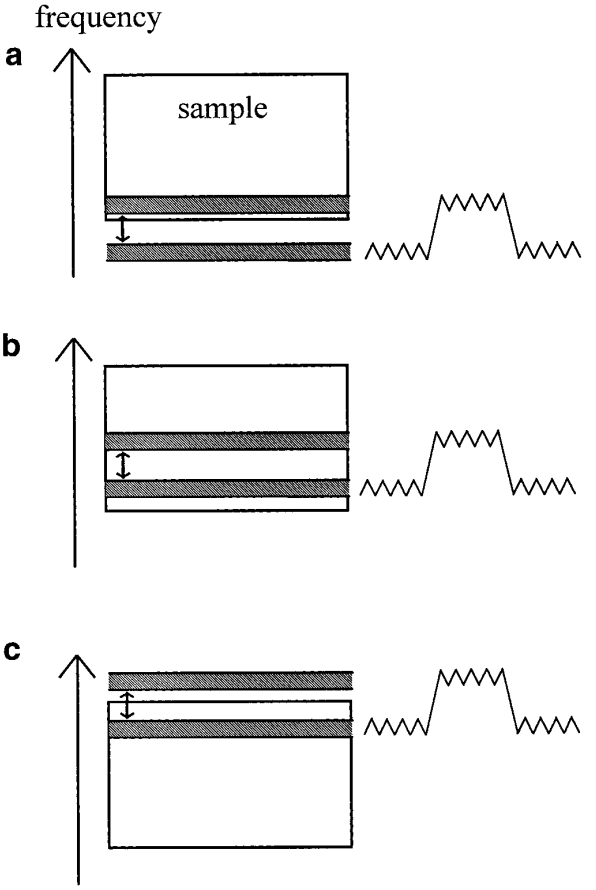

FIG. 3. The frequency distribution of the sample, together with the frequency bands of the FM-modulated RF. Three different situations are depicted which give one (a), two (b), and again one signal (c).

$$S_{\text{F}}^{1/2} = \sqrt{\frac{4kk_{\text{B}}T}{Q\omega_c}}, \qquad [4]$$

where k is the spring constant, T is the temperature, Q is the quality factor of the cantilever, and k_{B} is the Boltzmann constant. The quotient of the noise density at normal pressure and in a vacuum is approximately given by

$$\left(\frac{S_{\text{F,normal}}}{S_{\text{F,vacuum}}}\right)^{1/2} \approx \sqrt{\frac{Q_{\text{vacuum}}}{Q_{\text{normal}}}} \qquad [5]$$

under the assumption that the resonance frequency varies only slightly. Earlier measurements in a vacuum (*6*) were done with an effective Q on the order of 1000, so that our spectral noise density at room pressure is $\sqrt{10}$–$\sqrt{20}$ larger than these measurements. Since the signal should be independent of the ambient pressure, the signal-to-noise ratio has decreased by a factor of ≈4.

The modulation scheme for the T_1 measurements is shown

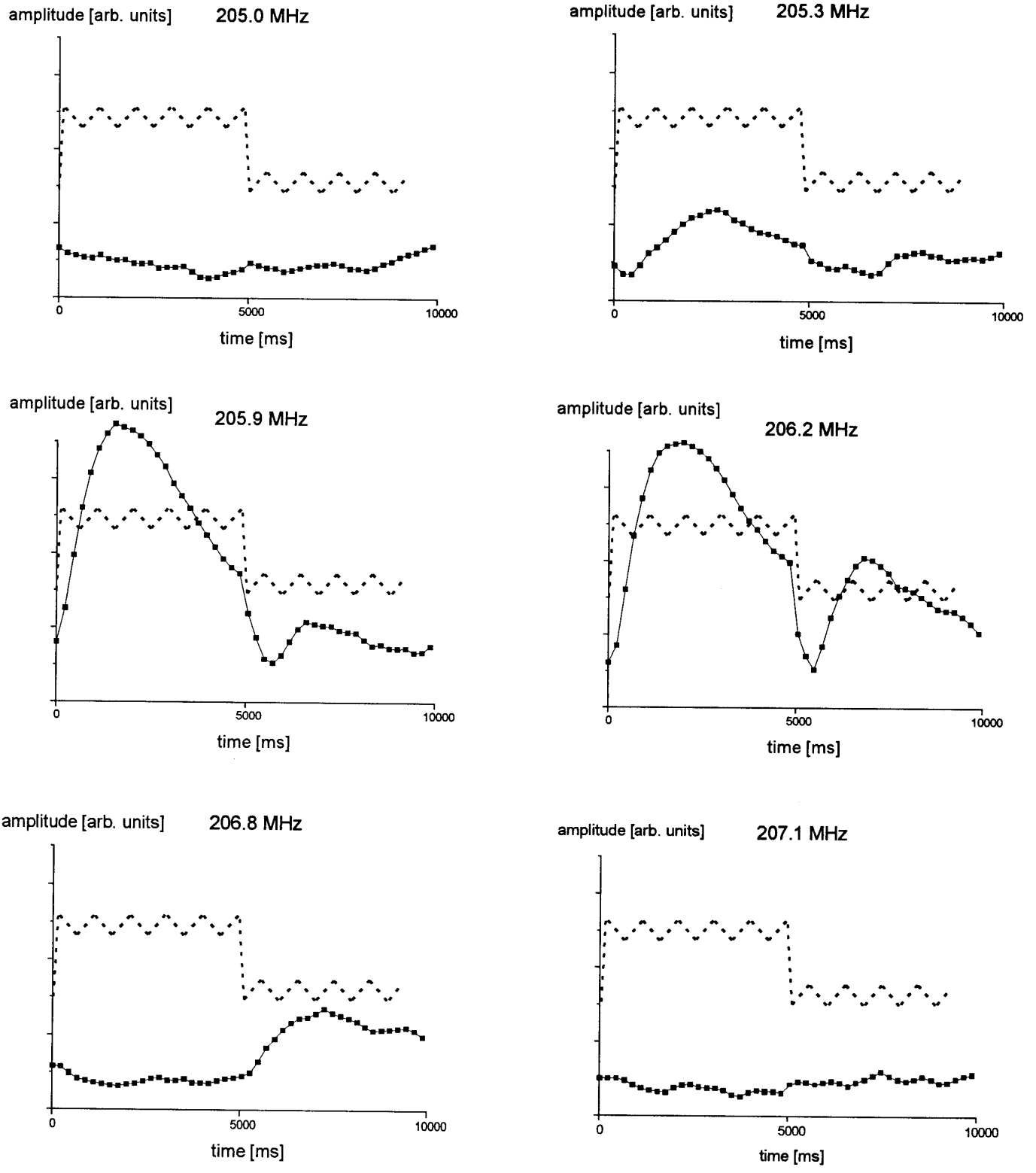

FIG. 4. MMR signals (connected points) produced by the modulation pattern of Fig. 2a for different RF center frequencies (each curve is the sum of 10 measurements). The FM-modulated, swept RF frequency is also shown. The first ramp occurs at $t = 0$ s, and the second at $t = 5$ s. The sample consisted of a grain of ammonium nitrate, the ramp depth was ± 500 kHz, the FM depth was ± 150 kHz, and the cantilever resonant frequency was 786 Hz. The lock-in time constant was 1 s.

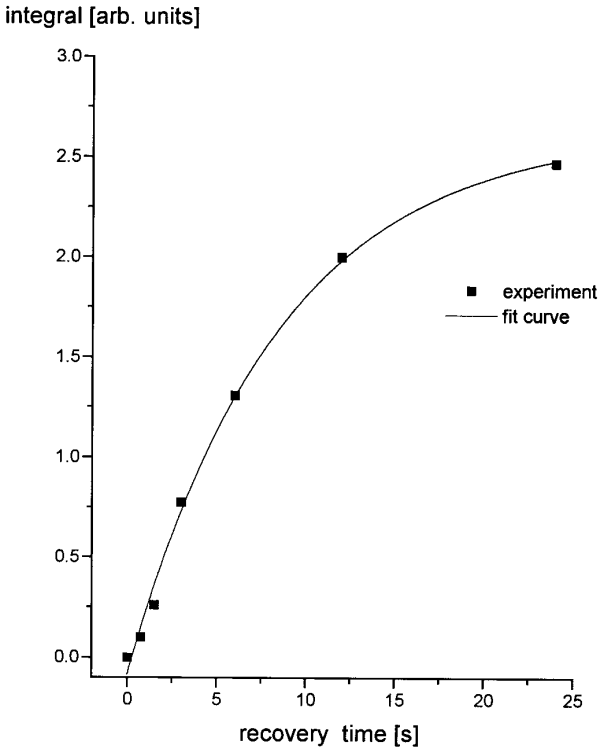

FIG. 5. The integrated signal intensity of a T_1 experiment for seven different recovery times (sum of 10 measurements). The sample consisted of ammonium nitrate, the cantilever resonant frequency was 527 Hz, the ramp depth was ±500 kHz, and the FM depth was ±150 kHz at a center frequency of 206.7 MHz.

in Fig. 2b. The idea is to destroy the magnetization completely during the saturation time. Then the RF is changed to a lower frequency which does not affect the spins and the magnetization can partially recover during the variable recovery time. The existing magnetization is then detected in the manner described previously.

The scheme for the $T_{1\rho}$ measurements (Fig. 2c) is similar to that in Fig. 2a, except for a variable time delay without FM between the end of the frequency ramp and the start of the frequency modulation. During this delay, the spin-locked magnetization decays with the $T_{1\rho}$ value of the region that has been spin-locked.

RESULTS AND DISCUSSION

Several experimental results of the excitation scheme of Fig. 2a with continuous frequency modulation are shown in Fig. 4. The figure shows the dc voltage output of the lock-in amplifier (sum of 10 experiments), which is proportional to the vibration amplitude of the cantilever, and the excitation frequency versus time; $t = 0$ corresponds to the start of the first ramp. The sample consisted of a grain of ammonium nitrate with typical dimensions of 70 μm. From the number of protons per unit volume ($N_p = 5.1 \times 10^{28}$ per cubic meter) the number of protons in the entire sample can be calculated to be 1.75×10^{16}, but due to the field gradient and the modulation depth, only a small slice of the sample contributes to the signal. The modulation depth of ±150 kHz and the field gradient of 500 T/m lead to a spatial excitation bandwidth of

$$\Delta z = \frac{\Delta B}{|\delta B_z/\delta z|} \approx 14\ \mu\text{m} \qquad [6]$$

in our experiment (which corresponds to 3.5×10^{15} protons), where ΔB is the effective NMR linewidth that is determined mainly by the frequency modulation. Shown are six measurements with different ω_{high} ranging from 205 to 207.1 MHz. The SNR can be determined by calculating the integral of the signal during the measurement time with and without spin signal. The constant offset has been neglected. The SNR in the experiment with the largest spin signal (205.9 MHz) is ≈900 for 10 scans and therefore 285 for 1

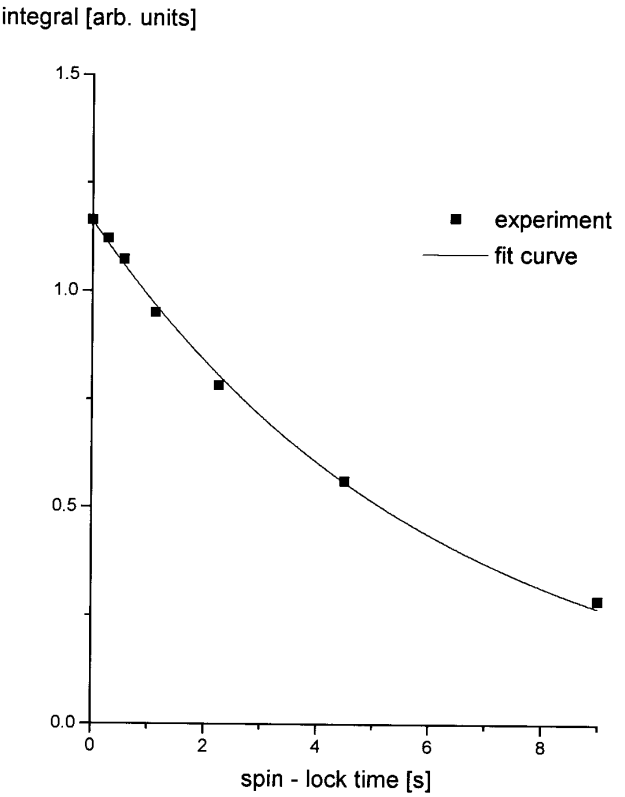

FIG. 6. The integrated signal intensity of a $T_{1\rho}$ experiment for seven different spin lock times (sum of 10 measurements). The sample consisted of ammonium sulfate, the cantilever resonant frequency was 600 Hz, the ramp depth was ±500 kHz, and the FM depth was ±150 kHz at a center frequency of 207 MHz.

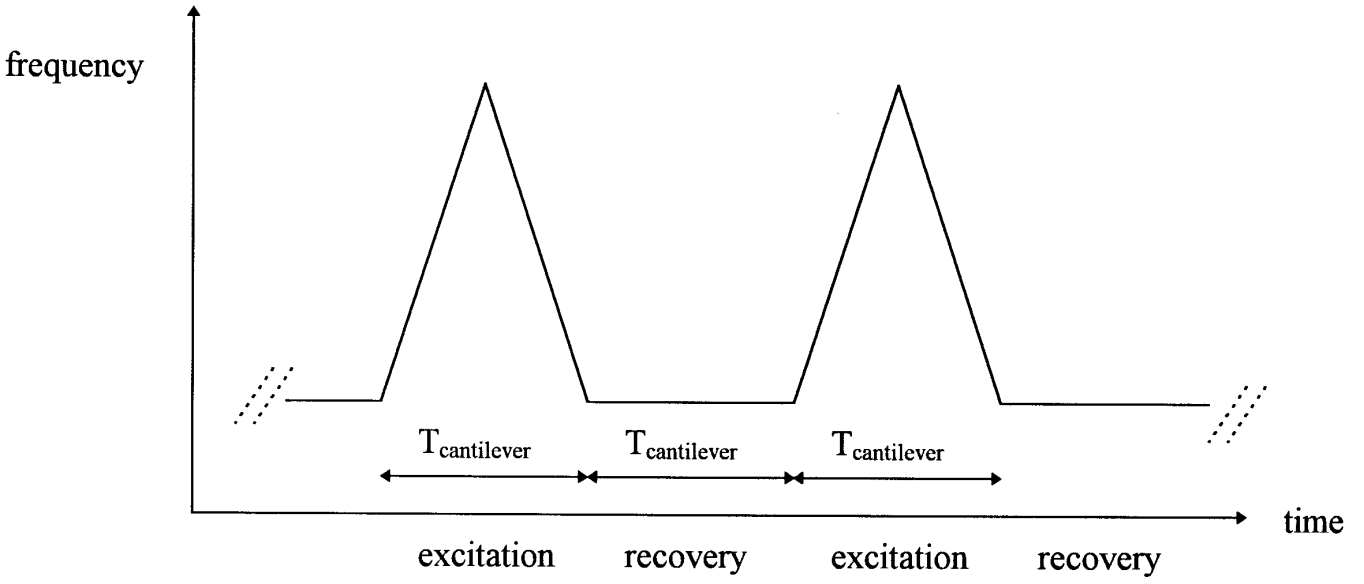

FIG. 7. Excitation pattern of the inversion-recovery detection method. The RF is ramped up and down in one resonant cantilever period, and then the magnetization can recover for one cantilever period. The depth of the ramps was ±500 kHz. This pattern is repeated continuously. Therefore, the magnetization oscillates around a steady-state value.

scan. From the calculation above one can determine the number of protons corresponding to unity SNR to be 1.2×10^{13} (1 scan). The minimum detectable slice size for the given ammonium nitrate particle would therefore be 49 nm, that is, far beyond the spatial z resolution calculated in our experiment. The corresponding voxel size is 6.2×10^{-6} m.

As discussed in the previous section one can expect up to two signals. With $\omega_{\text{high}} = 205.0$ MHz, both FM bands have center frequencies that are too low to excite any spins. By increasing ω_{high}, there first appears a signal after the first ramp, the situation of Fig. 3a, then two signals, the situation of Fig. 3b, then only a signal after the second ramp, Fig. 3c, and finally no signal for $\omega_{\text{high}} = 207.1$ MHz.

The appearance of a signal after the second ramp means that T_1 is not much longer than 5 s, the length of the period between the two ramps. T_1 cannot be much shorter than 5 s, because the second signal is smaller than the first.

The results of a T_1 measurement with the ammonium nitrate sample (typical dimensions 110 μm) are shown in Fig. 5. The integral of the signal (after the first ramp) of 10 measurements is plotted versus the recovery time (see also Fig. 2b). The points are fitted with the simple function

$$M(t) = M_{t=0}(1 - e^{-t/T_1}) \qquad [7]$$

with $T_1 = 8.5$ s.

The $T_{1\rho}$ experiments of Fig. 6 were carried out with a grain of ammonium sulfate (typical dimensions 110 μm). Similar to the T_1 experiment above, the integral of the signal of 10 measurements is plotted versus the spin-lock time (Fig. 2c). The fitting function is

$$M(t) = M_{t=0}e^{-t/T_{1\rho}}, \qquad [8]$$

which produces a $T_{1\rho}$ of 6.1 s. The value of $T_{1\rho}$ obtained by this method is not the one normally obtained with inductive NMR. Due to the field gradient, many spins in the sample are spin-locked off resonance. The offset frequency $B_0 \cdot \gamma - \omega_{\text{high}}$ affects $T_{1\rho}$ (*11*),

$$\frac{1}{T_{1\rho}} = \frac{1}{(B_0 - \omega_{\text{high}}/\gamma)^2 + B_{\text{RF}}^2}\left(\frac{(B_0 - \omega_{\text{high}}/\gamma)^2}{T_1} + \frac{B_{\text{RF}}^2}{T_{1\rho 0}}\right), \qquad [9]$$

where B_0 is the static field and $T_{1\rho 0}$ the relaxation time exactly on resonance. The effective value of $T_{1\rho}$ is between T_1 and $T_{1\rho 0}$. Due to the Larmor frequency distribution in the sample, the results of the MMR $T_{1\rho}$ measurements yield a $T_{1\rho}$ averaged over the region where the measurement takes place (roughly spoken, in the ±150 kHz region around the center frequency). The smaller the FM depth Ω, the more $T_{1\rho}$ equals $T_{1\rho 0}$.

Inversion-Recovery Measurement

The above experiments show that the proton $T_{1\rho}$ for ammonium sulfate and also for ammonium nitrate are relatively

long. This is why these compounds are chosen to demonstrate the MMR effect. For many samples at room temperature the proton $T_{1\rho}$ is much shorter than 1 s. A short $T_{1\rho}$ value causes the magnetization to decay during the many fast adiabatic passages, thereby decreasing the amplitude of the oscillating z magnetization and of the signal. For measurements at room temperature, other techniques that produce oscillating z magnetization need to be tested. The first method that comes to mind is the use of π pulses, spaced by a time equal to the oscillation period of the cantilever. This method has not been successful yet, because the π pulses directly excite the cantilever, mainly because of heat produced and mechanical vibrations of the RF coil. Also the normal pressure in the probe is favorable for the heat and sound transfer from coil to cantilever. In this respect, the fast passage method as first applied to nuclear MMR by Rugar *et al.* (*6*) is ideal, since the RF irradiation produces a constant effect on the cantilever.

We report some experiments with an inversion-recovery method. The modulation pattern is shown in Fig. 7. The frequency of the RF is swept up and down in one cantilever resonant period. Even with a very short $T_{1\rho}$ of 1–2 ms, enough magnetization remains to excite the cantilever during this single adiabatic cycle. Then a recovery period takes place for one cantilever period during which the magnetization repolarizes with T_1. Eventually a steady-state value of magnetization (and of the force), determined by T_1 and $T_{1\rho}$, will be reached. This method has been applied to ^{19}F at low temperatures (*7*). This method also functions at room temperature and at normal pressure, even for ammonium sulfate, where the long T_1 makes this method unfavorable. The results are shown in Fig. 8. The difference between the lock-in signal (average of 30 s) with and without excitation is plotted for five different RF frequencies. Also shown is the standard deviation of the signal with excitation. The signal reaches a maximum at $\approx$207.0 MHz. Tests with samples with much shorter T_1 and $T_{1\rho}$ are underway.

As a final conclusion, we remark that mechanically detected magnetic resonance experiments at room temperature and normal pressure are feasible, but to use them in a routine way for biological or other materials with short proton $T_{1\rho}$ values, the repetitive fast adiabatic passage method does not function well and other excitation schemes must be exploited.

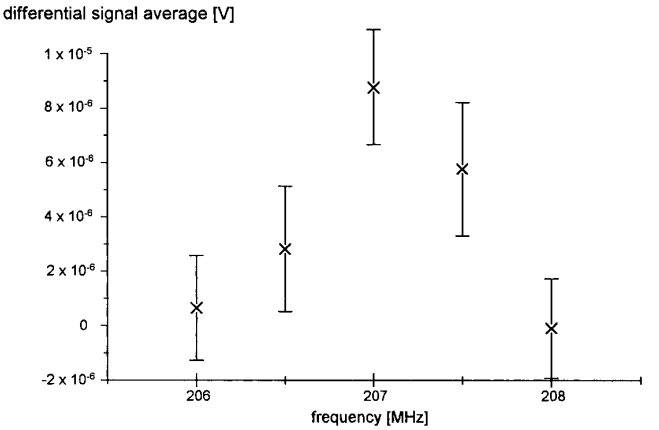

FIG. 8. Experimental results of the inversion-recovery experiment. The difference of the lock-in amplifier signal with and without modulation is plotted for five RF frequencies. Also shown is the standard deviation of the steady-state signal with modulation.

ACKNOWLEDGMENTS

We thank Dr. Dan Rugar and Professor Hans M. Vieth for helpful communication and the Studienstiftung des deutschen Volkes for a stipend for Arnd Schaff.

REFERENCES

1. J. A. Sidles, *Appl. Phys. Lett.* **58,** 2854 (1991).
2. J. A. Sidles, *Rev. Sci. Instrum.* **63,** 3881 (1992).
3. J. A. Sidles and D. Rugar, *Phys. Rev. Lett.* **70,** 3506 (1993).
4. D. Rugar, H. J. Mamin, and P. Guethner, *Appl. Phys. Lett.* **55,** 2588 (1989).
5. D. Rugar, C. S. Yannoni, and J. A. Sidles, *Nature* **360,** 563 (1992).
6. D. Rugar, O. Züger, S. Hoen, C. S. Yannoni, H. M. Vieth, and R. D. Kendrick, *Science* **264,** 1560 (1994).
7. K. Wago, O. Züger, R. Kendrick, C. S. Yannoni, and D. Rugar, *J. Vac. Sci. Technol. B* **14,** 1197 (1996).
8. O. Züger and D. Rugar, *Appl. Phys. Lett.* **63,** 2496 (1993).
9. O. Züger, S. T. Hoen, C. S. Yannoni, and D. Rugar, *J. Appl. Phys.* **79,** 1881 (1996).
10. C. P. Slichter, ''Principles of Magnetic Resonance,'' 2nd ed., p. 26, Springer-Verlag, Berlin/Heidelberg/New York, 1980.
11. C. P. Slichter, ''Principles of Magnetic Resonance,'' 2nd ed., Chap. 6.9, Springer-Verlag, Berlin/Heidelberg/New York, 1980.